JMEPEG (2020) 29:7445–7455
https://doi.org/10.1007/s11665-020-05197-8

1059-9495/$19.00

Elucidating the Effect of MoS_2 on the Mechanical and Tribological Behavior of AA7075/Si_3N_4 Composite

Mir Irfan Ul Haq, Ankush Raina, Ankush Anand, Sanjay Mohan Sharma, and Rajiv Kumar

(Submitted March 2, 2020; in revised form August 4, 2020; accepted September 24, 2020; published online October 19, 2020)

In the current work, a novel self-lubricating AA7075-based composite has been developed with silicon nitride (8 wt.%) as the ceramic reinforcement and varying MoS_2 (0-6 wt.%) content by using stir casting method. The effect of solid lubricant (MoS_2) addition on the microhardness, compression and microstructural behavior has been studied. Unidirectional sliding wear tests were carried out to study the effect of the reinforcement addition on the coefficient of friction and wear. The testing has been carried out at three different sliding speeds (1, 4 and 7 m/s) to elucidate the effect of sliding speed on the wear and friction behavior. The mechanical strength of the developed composites exhibited a decreasing trend with an increase in the MoS_2 content. However, a 37% decrease in the COF was also observed with an increase in molybdenum disulfide (MoS_2) content. With an increase in the normal load, COF exhibited an increasing behavior. The wear loss also exhibited an increasing trend with an increase in normal load as well as speed. The worn surface analysis exhibited a shift of wear mechanism from severe abrasion toward mild abrasion in the case of composites with higher content of MoS_2. EDS also revealed the formation of mechanically mixed layer (MML) and oxide formation. The developed composites with better anti-friction properties have wide scope in sliding applications, particularly in automotive sector.

Keywords AA7075, aluminum, friction, lightweight materials, MoS_2, self-lubricating composites, solid lubrication, stir casting, wear Si_3N_4

1. Introduction

The increasing demands for sustainable (Ref 1) technologies have led to an increased focus on the research in the area of lightweight materials such as aluminum and magnesium. Aluminum in its pure form lacks good mechanical properties and hence is not structurally much applicable. Aluminum when alloyed with various elements such as zinc, magnesium, silicon exhibits better mechanical properties. AA 7075 being an alloy of aluminum with zinc as the primary alloying element exhibits excellent mechanical properties comparable with steels; however, it offers less resistance to wear (Ref 2).

Friction and wear being intrinsic to various engineering applications, designers and material scientists are working on the development of materials with better mechanical properties along with good friction and wear properties. Due to the environmental, economic and technical disadvantages related to liquid lubrication, recently focus has shifted toward development of self-lubricating materials (Ref 3-5). In the case of self-lubricating materials, solid lubricants such as graphite, calcium fluoride, barium fluoride have been tried; however, adding the softer solid lubricant phase leads to a decrease in mechanical strength, thereby warranting the use of a hard ceramic reinforcement so as to counter the degradation of mechanical properties by the softer phase. Such composites with ceramic as the primary reinforcement and solid lubricant as the secondary reinforcement are known as hybrid self-lubricating composites.

In our previous work (Ref 4), silicon nitride was added as a reinforcement in AA7075 in varying percentages and the composites exhibited better hardness and wear resistance. The literature also revealed that silicon nitride, an excellent bearing material, has not been tried much as a reinforcement in the development of aluminum-based composites.

Vinoth et al. (Ref 6) studied the effect of MoS_2 addition on mechanical and tribological behavior of Al-Si10Mg alloy. The composites prepared via stir casting, as reported by the authors, a finer microstructure in the 4 wt.% MoS_2-added composites apart from increase in the density was observed. The fabricated composites with MoS_2 also exhibited better wear resistance with reference to the unreinforced alloy. However, the ultimate tensile strength decreased as compared to the base alloy. Furlan et al. (Ref 7) in a recent study summarized the role of MoS_2 as a solid lubricant in various base matrices such as copper, iron, nickel, aluminum and silver. The authors have summed and presented a detailed review of the various testing configurations, effect of environmental conditions and the various parameters on the friction and wear of MoS_2-added composites. The authors have summarized that MoS_2 plays a vital role in improving the tribological properties; however, the studies carried out in this direction are not much exhaustive. Lakshmipathy et al. (Ref 8) in a study examined the effect of MoS_2 on the mechanical and tribological behavior of AA7068 along with tungsten carbide (WC). The samples were, however, prepared via powder metallurgy technique. Kumar et al. (Ref 9) carried out an investigation wherein the authors studied the effect of addition of 4 wt.%MoS_2 to Al 10SiC on the tribological behavior. The samples were prepared via liquid metallurgy route. A decrease in the wear rate and coefficient of friction in the case of MoS_2-added composites was reported by

Mir Irfan Ul Haq, Ankush Raina, Ankush Anand, Sanjay Mohan Sharma, and **Rajiv Kumar**, School of Mechanical Engineering, SMVD University, Katra, Jammu and Kashmir 182320, India. Contact e-mail: haqmechanical@gmail.com.

the authors in comparison with the Al-SiC composites. The authors have attributed this improvement in the tribological properties of the composites to the film formation capability of MoS_2. Monikandan et al. (Ref 10) carried out a tribological study on AA6061-B_4C and AA6061-B_4C-MoS_2 composites. The samples were prepared via stir casting route. The authors carried out a statistical analysis wherein effect of various factors such as MoS_2 addition, load, sliding speed and sliding distance on the wear and friction behavior of the fabricated composites was studied. The authors concluded that with the increase in sliding distance and applied load, both wear rate and coefficient of friction showed an increasing trend, whereas MoS_2 particle addition led to a decrease in the wear rate as well as the coefficient of friction. Jojith and Radhika (Ref 11) carried out a study on LM13/TiO_2 (12 wt.%)/MoS_2 (3 wt.%) composites prepared via stir casting route. The authors reported an improvement in the hardness and tensile strength as compared to the base alloy. The authors reported an improvement in the wear resistance of the composites in comparison with the unreinforced alloy. Daniel et al. (Ref 12) studied the tribological behavior of Al/SiC/MoS_2 hybrid metal matrix composites under high-temperature conditions. They prepared the samples via casting route with AA 5059 as the base matrix and 2 wt.% MoS_2 as a constant solid lubricant additive and varied the ceramic reinforcement SiC. The authors documented that addition of SiC and MoS_2 led to a decrease in the wear as well as the coefficient of friction of the cast composites. The authors also concluded that temperature also affects the friction and wear behavior of the cast composites by a considerable amount. Kanthavel et al. (Ref 13) in a similar investigation studied the tribological properties on powder metallurgy-processed Al/Al_2O_3/MoS_2 hybrid composites. The authors reported that the combined effect of 5 wt.% Al_2O_3 and 5 wt.% MoS_2 exhibited better tribological performance. However, upon increasing the MoS_2 concentration to 10 wt.% the coefficient of friction exhibited a reverse trend.

In a recent study by the authors (Ref 5), the percentage of silicon nitride was fixed as 8 wt.% and graphite was varied in varying percentages. In view of the above discussion, it can be concluded that MoS_2 with excellent solid lubrication capabilities has not been tried with AA 7075. The current work was therefore aimed at studying the effect of MoS_2 addition on the tribological behavior of AA7075/Si_3N_4 composites. MoS_2 has been added in various percentages by weight (0, 2, 4, 6) while adding 8 wt.% silicon nitride to all the samples primarily on the basis of our previous work (Ref 4).

The literature (Ref 6, 11-15) suggests that very less efforts have been made toward development of AA7075-based self-lubricating composites with silicon nitride as the ceramic reinforcement. In our previous work (Ref 4, 5, 16), we studied the effect of silicon nitride and Gr on the tribological characteristics of AA7075-based composites. In the present work, a novel composite comprising of AA 7075 alloy as base matrix, Si_3N_4 particles as ceramic reinforcements (8 wt.%) and MoS_2 as the solid lubricant (0-6 wt.%) has been developed by stir casting route. The influence of MoS_2 on the mechanical and tribological behavior of AA 7075 has been investigated. The work attempts to exploit the potential of AA7075 as a promising engineering material owing to its better strength-to-weight ratio and further attempts to augment the good mechanical strength and anti-wear properties of Si_3N_4 and the good antifriction properties of MoS_2 so as to result in a composite with better mechanical and tribological properties.

2. Materials and Methods

2.1 Materials

Table 1 presents the details of the self-lubricating composites developed in the current study via stir casting method. Table 2 presents the properties of Si_3N_4 and molybdenum disulfide.

Figure 1 represents the XRD plots of AA7075/8 wt.% Si_3N_4 and AA7075/8 wt.% Si_3N_4/2 wt.% MoS_2 and AA7075/8 wt.% Si_3N_4/6 wt.% MoS_2. The increased height of the peaks in the case of the composites with MoS_2 at around $2\theta = 14.498°$ and around $2\theta = 39.66°$ confirms the presence of MoS_2 in the composites in addition to Si_3N_4 and AA7075.

2.2 Fabrication of Composites

Stir casting setup was used for the preparation of the composites. AA 7075 bar of 500 g was heated up to 950 °C in a graphite crucible by an electric furnace. The temperature was selected primarily to improve the wettability of the reinforcements, trail testing and on the basis of prior literature (Ref 17-19). The reinforcing particles were preheated prior to addition into the metal. Stirring was carried by a motorized stirrer to ensure homogenous mixing of the reinforcements (Ref 17). Various process parameters used in the stir casting process are presented in Table 3. The molten composite was allowed to flow into a preheated permanent mold which allowed to cool at room temperature thereafter. The castings were then machined on a lathe machine (HMT Make) to form cylindrical pins of required dimensions as per the testing procedures.

2.3 Mechanical and Tribological Testing

Archimedes principle was used to measure the density of the composites. The microhardness measurement was carried out using Vickers hardness tester (Daksh Quality Systems) according to ASTM E92 standard. The hardness tester is computer-enabled with image analysis software having an automatic turret with a testing range of force up to 100 gms having a magnification range of 100× to 400× and the dwell time range from 1 to 99 s. The indentation load for all tests was 5 N with a constant dwell time of 5 s. Microhardness of each composition was measured at five different locations, and three samples per composition were tested to ensure repeatability of the results.

The compression testing was carried out on samples with 10 mm diameter and 15 mm height (L/D ratio = 1.5) using a Universal Testing Machine (UTM) with constant velocity according to ASTM E9 standard. The compression testing for all compositions was performed three times to ensure repeatability.

The tribological studies were carried out on a computer-integrated pin-on-disk tribometer (DUCOM Wear and Friction Monitor TR-20LE-PHM400) with an inbuilt load cell to measure the frictional force, having a load range up to 200 N, RPM up to 2000 RPM and frictional force measurement range up to 200 N. Cylindrical pins of the cast composites with 8 mm diameter and 8 mm height were used for tribological testing.

A steel disk of EN 31 steel with a hardness value of around 60 ± 3 HRC was used as the counterface material. The tribotesting was carried out at five different normal loads (10, 20, 30, 40 and 50 N). The sliding was carried up to a distance of 1500 meters at a constant sliding speed of 1 m/s. In

Table 1 Details of AA 7075/Si_3N_4/MoS_2 composites

S. no.	AA 7075, wt.%	Si_3N_4, wt.%	Molybdenum disulfide, wt.%
1	Remaining	8	0
2	Remaining	8	2
3	Remaining	8	4
4	Remaining	8	6

Table 2 Details of reinforcing particles

Material	Appearance	Purity	Average particle size	Density	Supplier name
Silicon nitride	Gray white powder	> 99%	< 40 µm	3.52 g/cm^3	Nanopar Tech (Chandigarh, India)
Molybdenum disulfide	Silvery black	~ 99.9%	~ 44 µm	5.06 g/cm^3	Nanoshel Ltd (India)

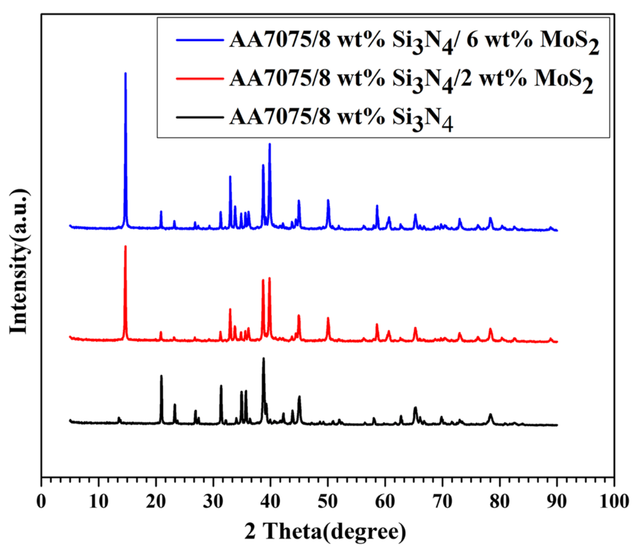

Fig. 1 XRD plot of AA7075/Si_3N_4/MoS_2 composites

Table 3 Process parameters used in stir casting

S. no.	Parameter	Value
1	Temperature during stirring	950 °C
2	RPM of the motor	250 RPM
3	Time for stirring	10 Min
4	Preheating temperature of reinforcing powders	450 °C
5	Preheating temperature for permanent mold	300 °C

order to study the effect of sliding speed on the friction and wear behavior of the developed composites, the testing was carried out at three different sliding speeds (1, 4 and 7 m/s) at a constant load of 30 N.

The tribological testing was carried out at room temperature. Prior to every test, polishing of the samples was performed by different grades of silicon carbide emery papers on a motorized polishing machine to ensure similar surface roughness conditions (Ra value of around 0.3 µm). The polishing machine is equipped with a polishing disk of 200 mm diameter made up of gun metal, having a speed variation of 300-900 RPM.

Acetone-cleaned samples were weighed by using an electronic weighing balance (Denver Instrument, Model SI 234) with an accuracy of 10^{-4} g as shown in Fig. 3.19. The wear loss was reported as a difference in weight of the samples measured before and after each test. Each experiment was repeated thrice, and an average value is reported. Scanning electron microscopy (SEM) and EDS analysis were performed to analyze the worn surfaces and elemental analysis, respectively. For evaluating the effect of various reinforcements on the microstructure of the developed composites, the microstructural analysis was carried under a scanning electron microscope equipped with energy-dispersive analysis (EDS) (FEI Quanta 200). Prior to the microstructural examination, the properly polished samples were etched by Keller's reagent (95 mL water +2.5 mL HNO3 +1.5 mL HCl +1.0 mL HF). Scanning electron microscope (JEOL JSM 5600 LV) was used to evaluate the type of wear mechanism after the tribological testing. EDS was used for chemical examination of the samples.

3. Results and Discussion

3.1 Mechanical Testing

3.1.1 Microhardness and Density. The density of the composites is presented in Table 4 wherein it can be seen that the density of the composites increases with an increase in the MoS_2 content. This is primarily due to the higher density of the MoS_2 particles. Figure 2 represents the microhardness values of the developed composites wherein it can be seen that the microhardness decreases with an increase in the MoS_2 content.

Table 4 Density of $AA7075/Si_3N_4/MoS_2$ composites

S. no.	Composition	Experimental density
1	AA7075/8 wt.% Si_3N_4	2.90
2	AA7075/8 wt.% Si_3N_4/2 wt.% MoS_2	2.91
3	AA7075/8 wt.% Si_3N_4/4 wt.% MoS_2	2.93
4	AA7075/8 wt.% Si_3N_4/6 wt.% MoS_2	2.98

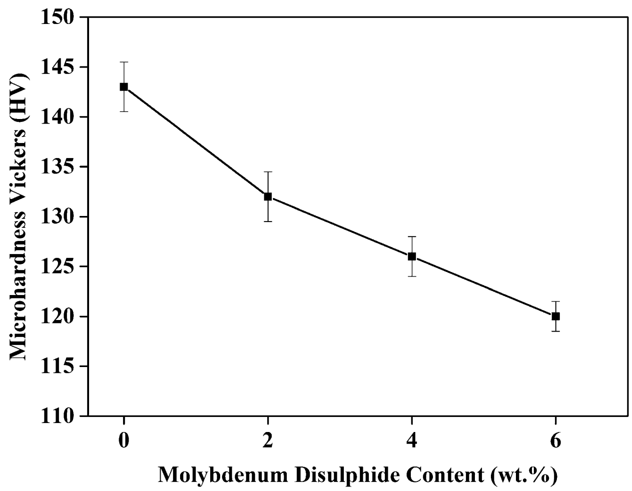

Fig. 2 Effect of molybdenum disulfide content on microhardness

The microhardness value drops from around 143 HV for the ceramic-reinforced composite (8 wt.%) to around 120 HV for the self-lubricating composite with 6 wt.% MoS_2 (Ref 20) .

The increase in the softer MoS_2 particles leads to this behavior. Moreover, the softer MoS_2 phase promotes easy movement of grains in the direction of slip planes, which further renders the material more susceptible to deformation under load (Ref 21). Figure 3 shows the representative microstructural images of the cast composites. The microstructural changes and clustering of particles triggered by the MoS_2 particles also contribute to the decrease in the microhardness (Ref 22). The addition of Si_3N_4 leads to grain refinement as observed in our previous work (Ref 4) due to Hall–Petch effect and is instrumental in improving the hardness and wear resistance of the composite in comparison with the base alloy (Ref 23). However, it was observed that addition of the softer MoS_2 particles counters this effect of grain refinement, which in turn leads to decrease in microhardness in comparison with the AA7075/Si3N4 composites. It is evident from Fig. 2 that the decrease in the microhardness in the case of MoS_2 composites is more in comparison with the graphitic composites studied in our previous work (Ref 5).

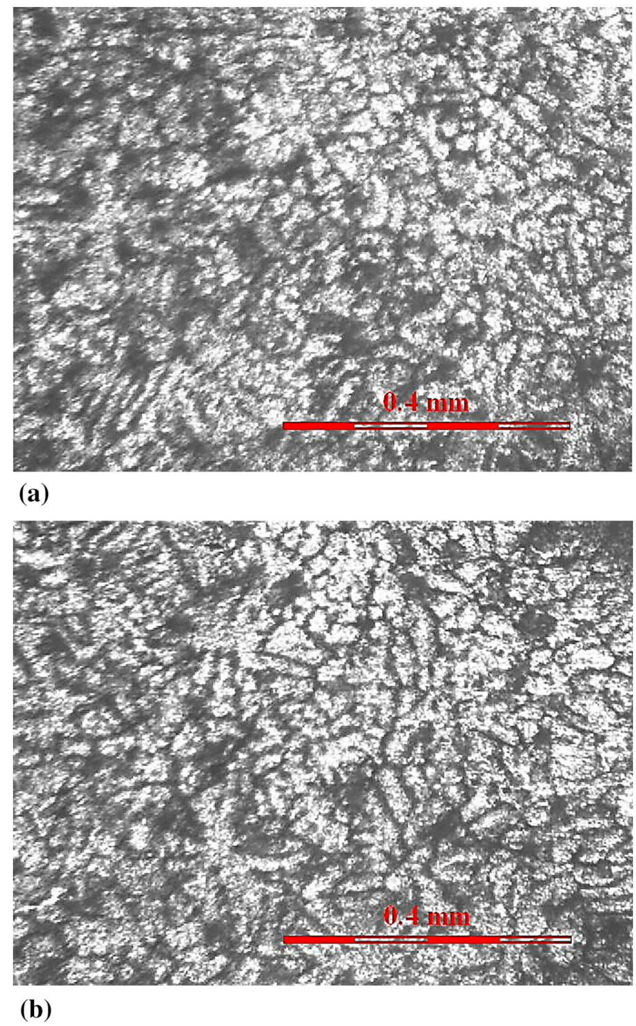

Fig. 3 Representative microstructural image of (a) AA7075/8 wt.% Si_3N_4/2 wt.% MoS_2 (b) AA7075/8 wt.% Si_3N_4/6 wt.% MoS_2 composites

3.1.2 Compression Testing. The results of the compression testing are presented in Fig. 4. The compression strength for the MoS_2 composites, which is a very critical property for prospective tribological materials, is higher than the base alloy (AA 7075). This behavior plays a vital role in improving the wear resistance of the developed composites. It can be observed that the addition of the MoS_2 particles leads to a decrease in the compression strength which can be ascribed to the relatively soft nature of the MoS_2 particles. The increased concentration of the particles also aids in the crack initiation at the matrix–reinforcement interface, thereby leading to the degradation of the mechanical properties (Ref 24). The decrease in the

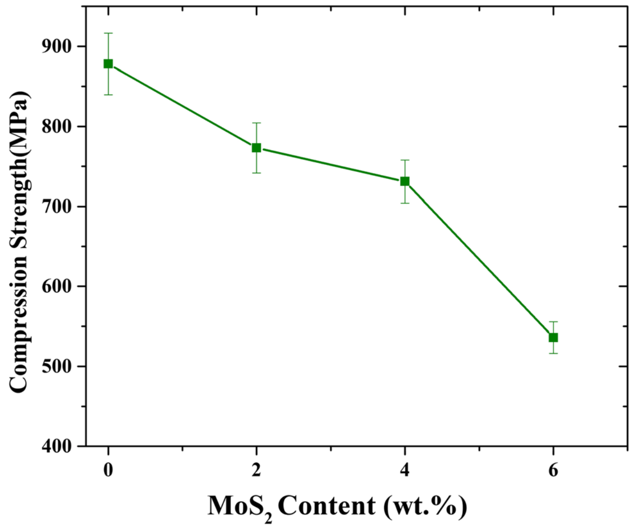

Fig. 4 Effect of molybdenum disulfide content on compression strength

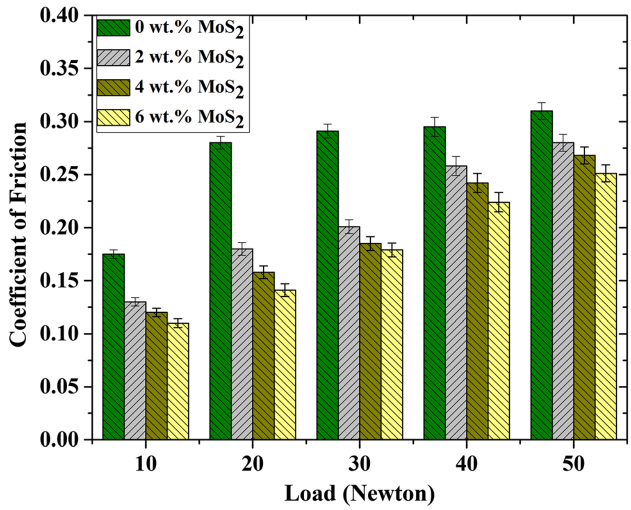

Fig. 5 Effect of molybdenum disulfide content on COF

compression strength is more than the graphitic composites (Ref 5), which is due to the softer MoS_2 phase as compared to graphite.

3.2 Tribological Testing

3.2.1 Effect of MoS_2 on COF. Figure 5 shows that an increase in the MoS_2 content leads to a decrease in the COF. A reduction of around 40% is achieved in the case of 6 wt.% MoS_2 composites in comparison with 0 wt.% composites at low load; however, the reduction is less in the case of higher loads. This behavior is attributed to tribofilm formation nature of MoS_2 (Ref 25). The MoS_2 tribofilm prevents the asperity to asperity contact, thereby lowering the COF. Moreover, the MoS_2 particles present in the debris also contribute to this behavior (Ref 26). A shift in the wear mechanism from abrasion (seen in the form of plowing marks) to a combination of delamination and milder abrasion also contributes to this behavior (Fig. 15a, 16a, 17a and 18a). Similar behavior has

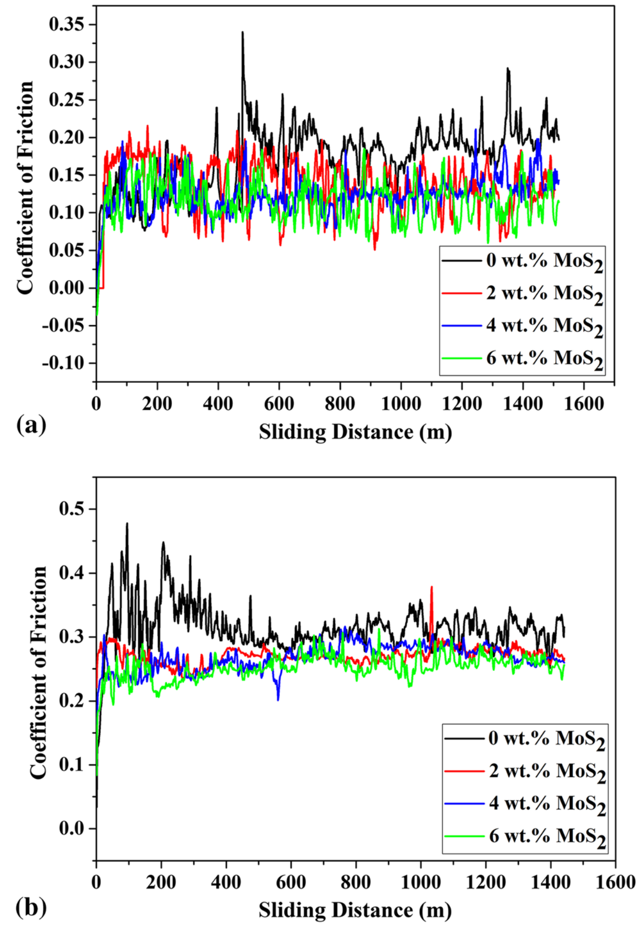

Fig. 6 Frictional characteristics of AA7075/Si_3N_4/MoS_2 at 1 m/s: a) at 10 N load and b) 50 N load

been observed in the case of AA7075/Si_3N_4/Gr composites (Ref 5). It can further be seen that in comparison with composites with graphite, MoS_2 is more efficient in lowering friction. This is primarily due to better film formation capability of MoS_2 in comparison with graphite (Ref 27). A shift in the wear mechanism from severe abrasion (with deeper grooves) toward mild abrasion (with smoother grooves) also contributes to this trend. The lubrication capability of MoS_2 is attributed to the chemical structure of the MoS_2, due to which shearing of the basal planes takes place in the direction of sliding (Ref 28). The promising results exhibited by MoS_2 hold more relevance for space and aerospace applications due to two reasons: (a) MoS_2 performs better than graphite as a solid lubricant in vacuum as graphite requires sufficient vapor pressure to perform efficiently (Ref 29) and (b) the base alloy AA7075 is an aerospace alloy which is widely used for space applications (Ref 30).

3.3 Effect of Load on COF

The friction curves corresponding to 10 and 50 N load and 1 m/s are presented in Fig. 6(a) and (b), respectively. In general, an initial increase is observed and after around 200 m and 250 m sliding, the friction curve stabilizes for 10 and 50 N load, respectively. This behavior is attributed to the breaking of asperities and increase in the real area of contact. The sharp peaks observed in the friction curves are due to third-body abrasion or due to breaking of the protective film. As evident from Fig. 6(a) and (b), comparatively stable curves can be observed in the case of 50 N load in comparison with 10 N load. Further, it can be observed that at lower loads, MoS_2 is more effective in lowering friction than at higher loads.

Figure 5 shows that with an increase in the normal load, the COF increases. This increase in the COF may be attributed to the increased locking of the asperities due to increase in the contact pressure. The breaking of the tribofilm/solid lubricant film due to an increase in the contact pressure also leads to an increase in COF (Ref 31). In the case of MoS_2 composites, it was observed that the increase in COF is sharp at low loads (10, 20 N), compared to an increase at higher loads (40 N, 50 N). A similar trend for the graphitic composites was also observed which is primarily due to the similarity in the chemical structure and solid lubrication mechanism of graphite and MoS_2 (Ref 32). An increase in the interface temperature at the higher loads leads to softening of the material at the interface and thereby increases the chances of adhesion (Ref 33). This behavior also contributes to the increase in the COF.

3.4 Influence of Speed on COF

The friction curves of different composites corresponding to 1, 4 and 7 m/s at a constant load of 30 N are presented in Fig. 7, 8, and 9, respectively. The steady state in the case of 1 and 4 m/s is reached at around 200 m as against 300 m in the case of 7 m/s. Smoother curves corresponding to 4 and 7 m/s are observed in comparison with 1 m/s. This behavior suggests that MoS_2 is a good candidate as a solid lubricant additive for higher speeds also. In addition to this, stable curves are observed in the case of composites with MoS_2 content in comparison with 0 wt.% MoS_2 composites. This behavior may be attributed to the lubricity of MoS_2.

Figure 10 shows that with a rise in the sliding speed, the COF decreases. This decrease is due to softening of the material due to frictional heating at the tribocontact. Some researchers have opined that higher temperature results in oxide formation. The oxide formed therein results in lower COF.

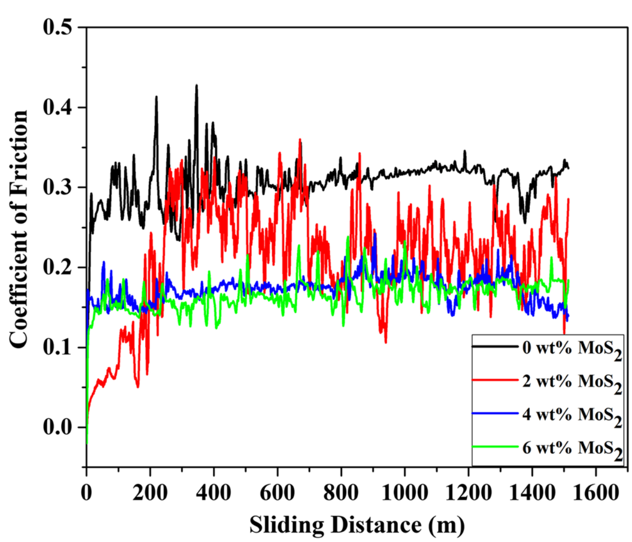

Fig. 7 Friction characteristics corresponding to speed of 1 m/s at 30 N

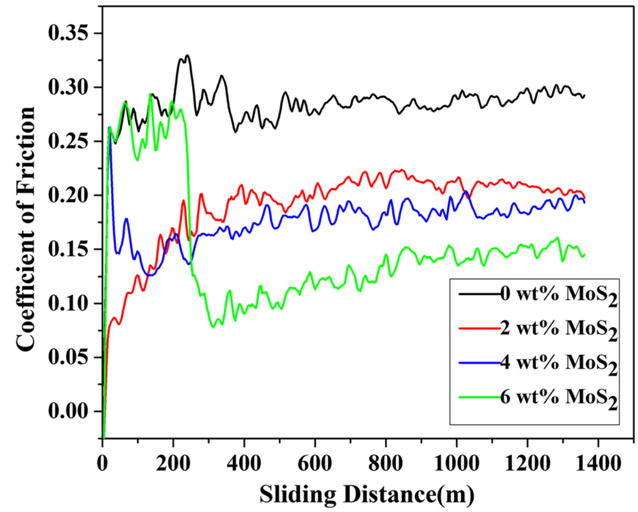

Fig. 8 Friction characteristics corresponding to speed of 4 m/s at 30 N

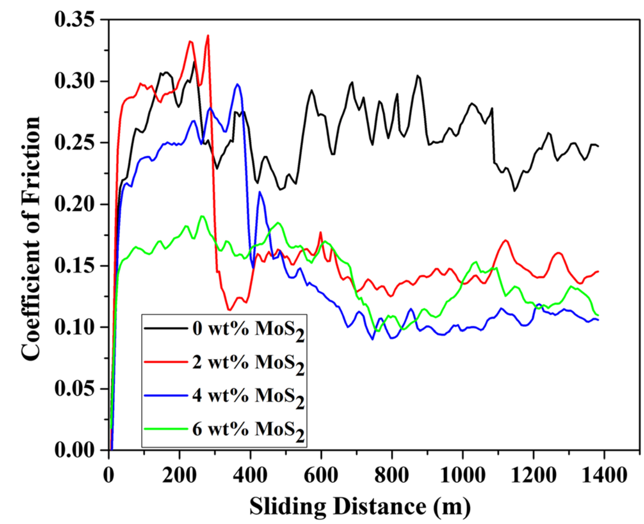

Fig. 9 Friction characteristics corresponding to speed of 7 m/s at 30 N

3.5 Effect of MoS_2 on Wear

The wear loss is a function of microhardness of the composites and the film formation capability of MoS_2. It can be observed from Fig. 2 that the microhardness decreases with an addition of the MoS_2. The decrease in microhardness leads to a decrease in the wear resistance, whereas the film formation capability improves the wear resistance as the solid lubricant film prevents the direct contact between the sliding surfaces and prevents further removal of material. It can be concluded that the film formation capability of MoS_2 dominates the effect caused by decrease in the microhardness (Ref 20) leading to an overall increase in the wear resistance. Figure 11 shows that for all compositions with MoS_2, the wear loss decreases; however, at low loads (10 and 20 N), 2wt.% MoS_2 is enough to form a film and wear loss is least at 2 wt.% MoS_2. Contrary to this, at higher loads (40 N and 50 N), it can be concluded that due to higher contact pressure, 2 wt.% MoS_2 is not sufficient to form a stable film; therefore, the composites with 4 wt.% MoS_2 exhibit

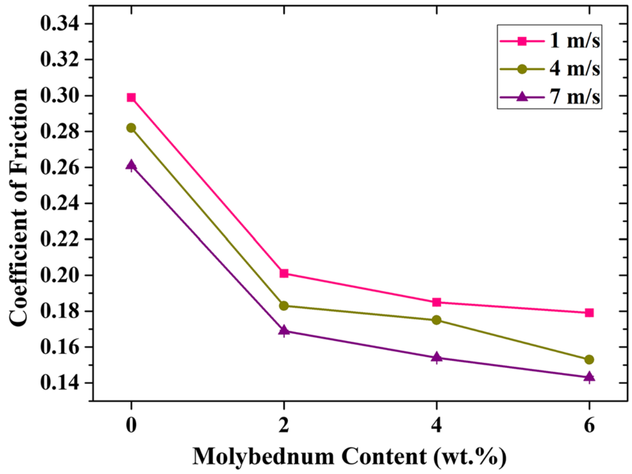

Fig. 10 Influence of speed on coefficient of friction (COF)

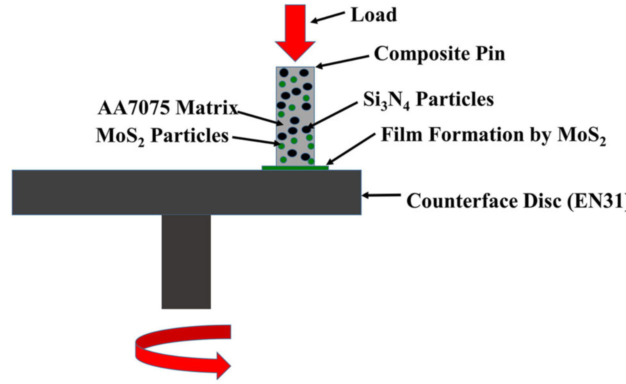

Fig. 12 Schematic representation of the mechanism of lubrication and the tribopair

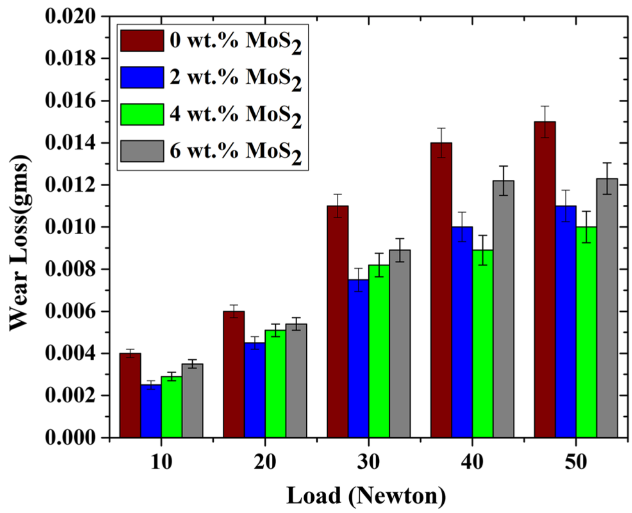

Fig. 11 Effect of molybdenum disulfide content on wear loss

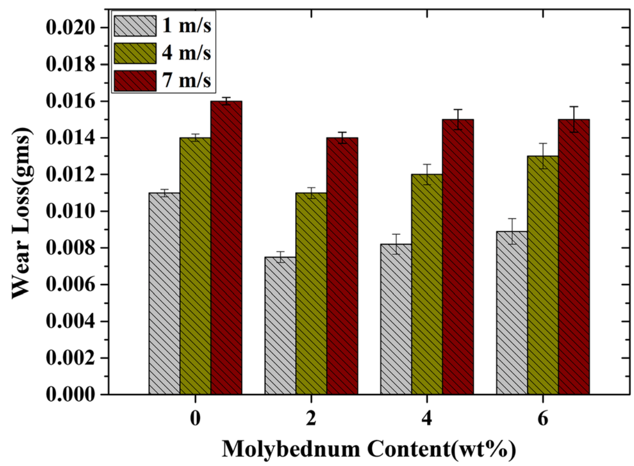

Fig. 13 Influence of sliding speed on wear loss

better wear resistance. The schematic representation presented in Fig. 12 shows the mechanism of the MoS_2 added in the composite in improving the tribological properties. The MoS_2 particles coming out in the form of wear particles get adhered to the counterface and aid in the film formation.

3.6 Effect of Load on Wear

From Fig. 11, it is clear that the increase in load leads to an increase in the wear loss for all the composites. This increase in the wear loss is in accordance with the Archard's wear law (Archard 1953). This behavior may be attributed to the breaking of the asperities and thereby increasing material loss. The increase in the load leads to the penetration of harder counterface into the softer pin material. Moreover, the subsurface crack initiation also triggers material delamination (Ref 34). The increase in contact pressure also leads to softening of the material. This softening leads to more material loss (Ref 35). A transition in the behavior can be clearly seen at 30 N load as in the case of 10 and 20 N loads the minimum wear loss is exhibited by 2 wt.% MoS_2 whereas in the case of 40 N and 50 N 4 wt.% MoS_2 exhibits the minimum wear loss. Higher loads result in breaking of tribolayers; hence, the effectiveness of the solid lubricant is lowered in improving the wear resistance.

3.7 Influence of Speed on Wear

Figure 13 shows the wear behavior at different speeds wherein it can be seen that the wear rises with an increase in speed. This effect may be attributed to the rise in the plastic deformation in the sliding direction due to rise in the speed. This plastic deformation leads to material delamination and thereby increase in the wear loss. The thermal softening due to an increase in the interfacial temperature also contributes to the increased wear loss. Moreover, deeper plowing and delamination marks can also be observed in the case of higher speeds from SEM analysis. The SEM analysis further suggests a transition in the wear mechanism from mild to severe. The delamination pits also act as active sites of progressive wear. Also during sliding at higher speeds, when the interface temperature crosses the critical temperature, the tribolayers over the softer bulk material are damaged during sliding, which renders the material in direct contact with the counterface. Further, a new layer formation over a relatively hotter and softer matrix becomes difficult (Ref 36).

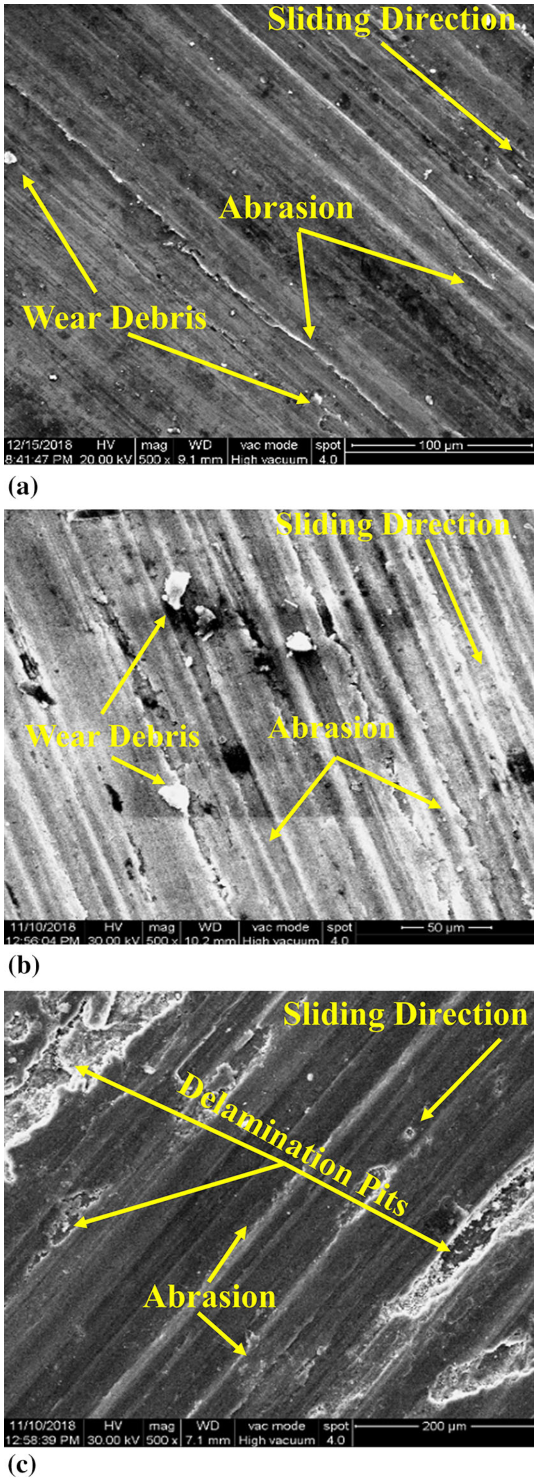

Fig. 14 SEM image of worn samples of AA7075/8 wt.% Si_3N_4 composite at (a) 1 m/s, (b) 4 m/s, (c)7 m/s corresponding to 30 N load

3.8 Worn Surface Analysis

Figure 14, 15, 16 and 17 presents the SEM images of the different composites corresponding to different sliding speeds. It can be seen from Fig. 14 that in the case of composites with 8 wt.% Si_3N_4 abrasion is the dominant wear mechanism and the severity of the abrasion marks increases as the speed increases.

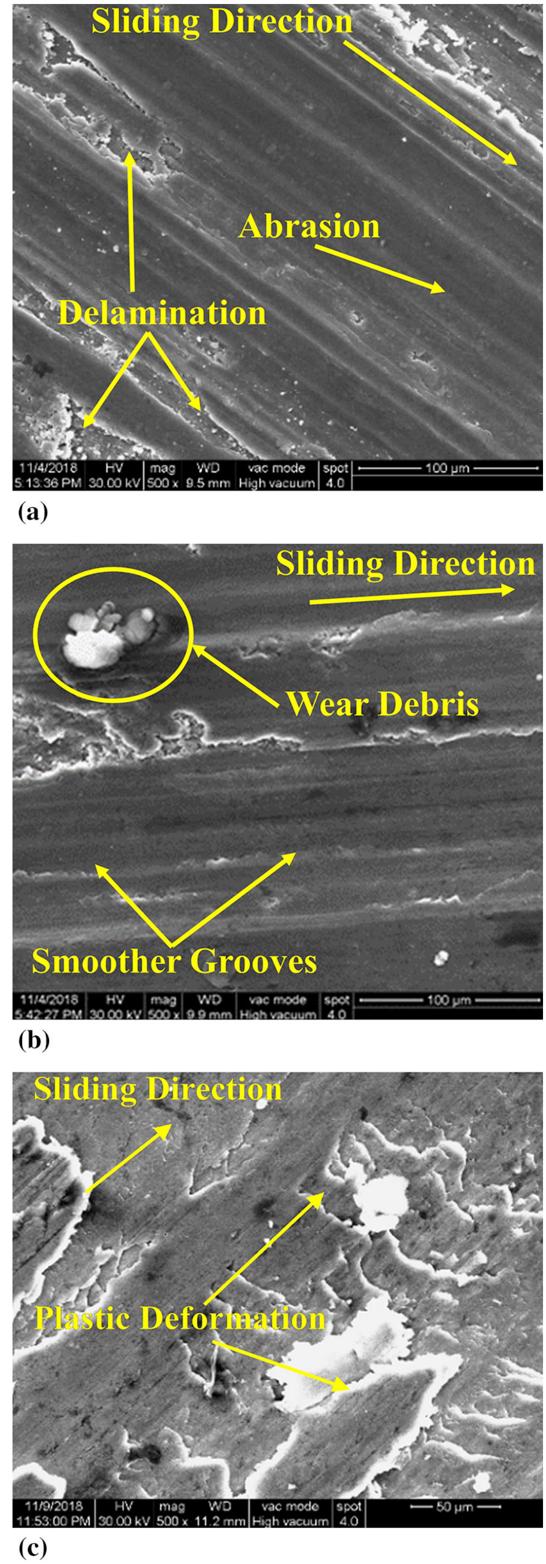

Fig. 15 SEM image of worn samples of AA7075/8 wt.% Si_3N_4/2 wt.% MoS_2 composite at (a) 1 m/s (b) 4 m/s (c)7 m/s corresponding to 30 N load

In the case of the composites with 2 wt.% MoS_2 (Fig. 15), it can be seen that a combined mild abrasion and delamination wear mechanisms are prevalent. It can also be seen from Fig. 15 and 16 that as the percentage of MoS_2 in the composites

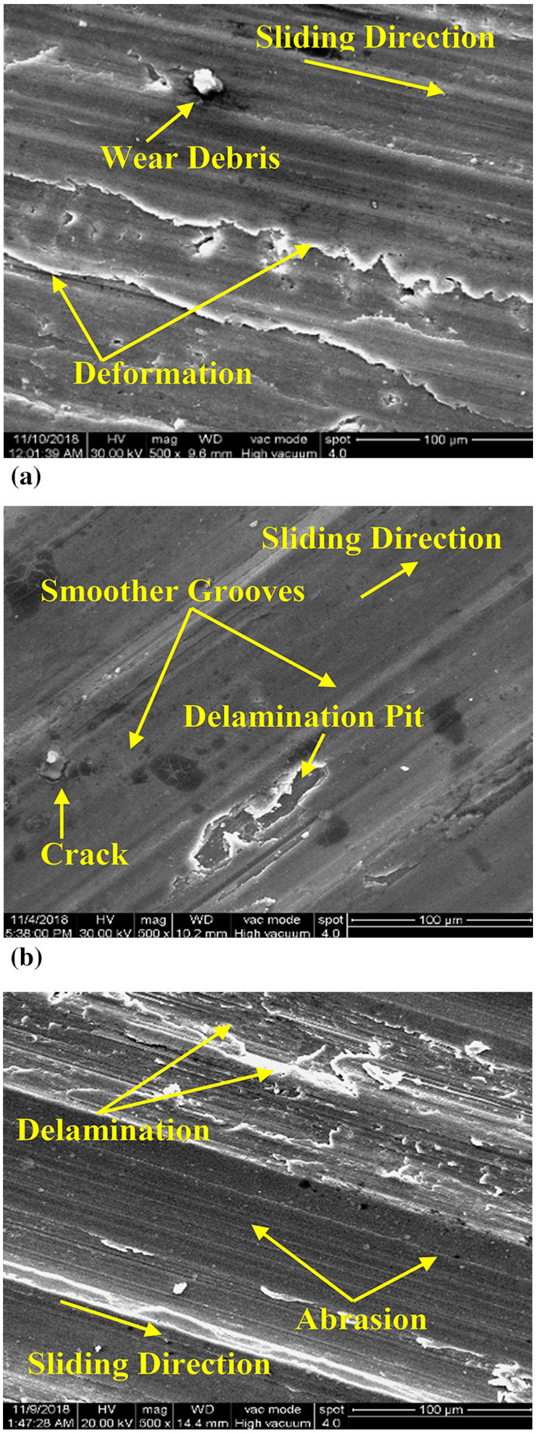

Fig. 16 SEM image of worn samples of AA7075/8 wt.% Si_3N_4/4 wt.% MoS_2 composite at (a) 1 m/s, (b) 4 m/s, (c)7 m/s corresponding to 30 N load

increases, the wear mechanism changes from abrasion toward delamination. It can also be observed that an increase in the MoS_2 content leads to the smoothening of the worn-out grooves at all speeds. It can be observed that an increase in speed leads to an increase in the depth of the grooves and the plastic deformation in the direction of the sliding. Some mild cracks can also be observed, which act as sites of material loss.

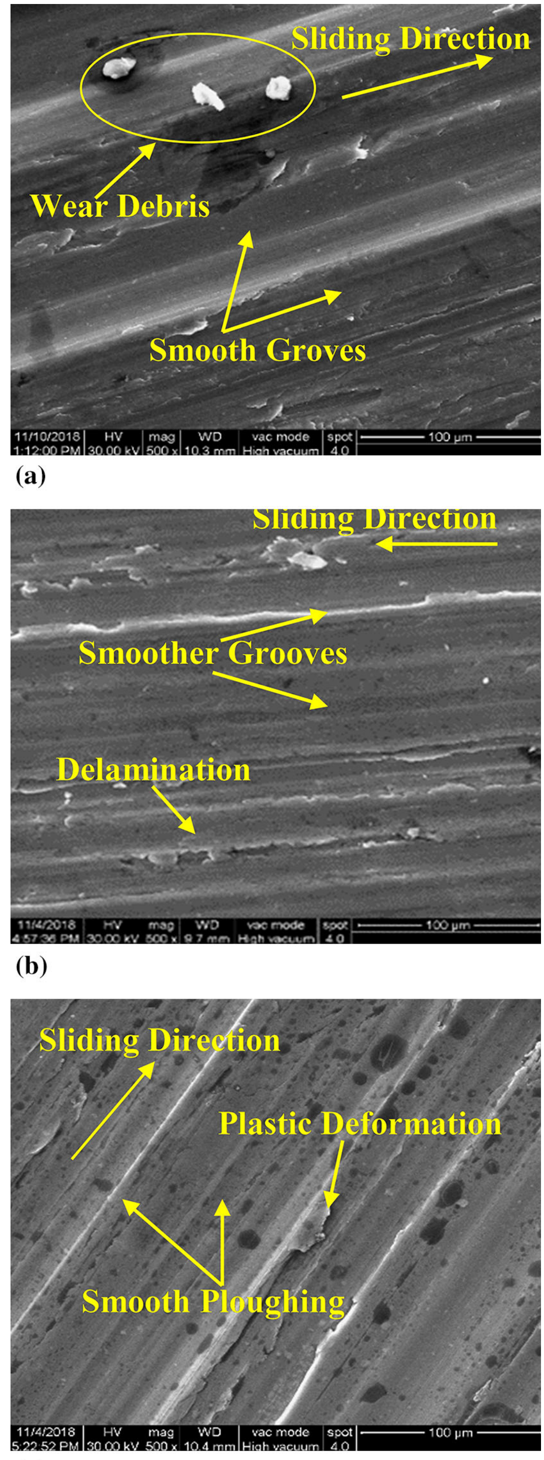

Fig. 17 SEM image of worn samples of AA7075/8 wt.% Si_3N_4/6 wt.% MoS_2 composite at (a) 1 m/s, (b) 4 m/s, (c) 7 m/s corresponding to 30 N load

This behavior shows that MoS_2 plays a significant role in lowering the COF. This is primarily due to lubricity of MoS_2. Some wear debris can also be seen in the worn surfaces as indicated in the images. Figure 18 presents EDS of the worn-out sample, which indicates the oxide formation and mechanically mixed layer (MML) formation. The traces of the counterbody material (Fe) in the EDS of the worn sample

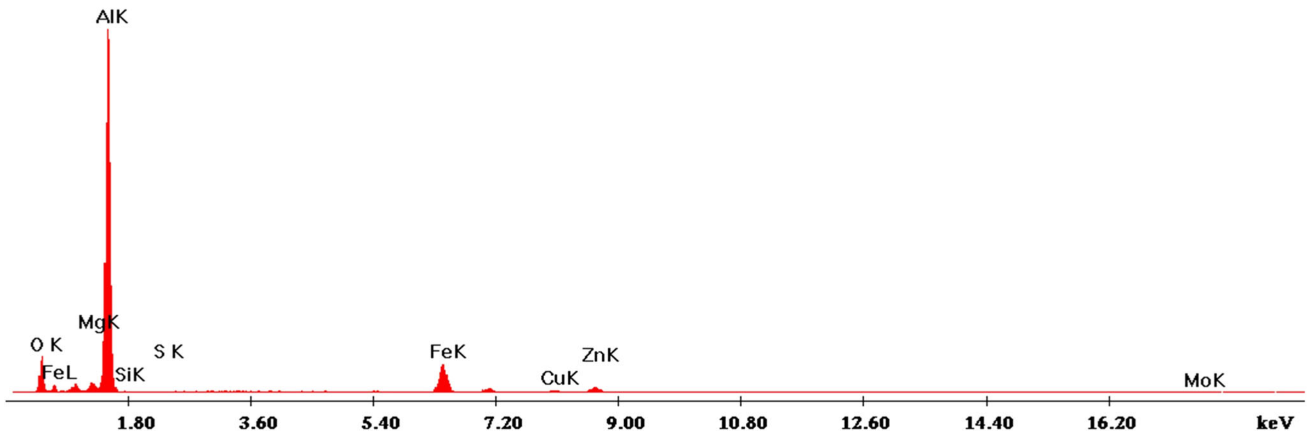

Fig. 18 EDS image of AA7075/Si_3N_4/2wt.% MoS_2 worn-out sample

suggest a transfer of material from the countersurface. Further, the piercing of the sharper wear debris particles into the softer pin also aids in the formation of MML. The MML aids in lowering friction and improving the wear resistance by preventing metal-to-metal contact (Ref 37).

4. Conclusions

AA7075/Si_3N_4/MoS_2-based composites have been successfully cast. The density of the developed composites increased with an increase in the MoS_2 content. The mechanical properties of the developed composites exhibited a decreasing trend with a 16% decrease in the microhardness and a 36% decrease in the compression strength. A 37% decrease in the COF was also observed with an increase in molybdenum disulfide (MoS_2) content. This decrease in the COF is more in comparison with composites with graphite as the solid lubricant. With an increase in the normal load, COF exhibited an increasing behavior.

The wear loss also exhibited an increasing trend with an increase in normal load as well as speed. The composites with 2 wt.% MoS_2 exhibited minimum wear loss at lower loads, whereas in the case of higher loads 4 wt.% MoS_2 exhibited minimum wear loss. The worn surface analysis exhibited a shift of wear mechanism from severe abrasion toward mild abrasion in the case of composites with higher content of MoS_2. EDS also revealed the formation of mechanically mixed layer (MML) and oxide formation. The testing revealed that the developed composites could serve various sliding wear applications wherein higher sliding speeds are prevalent.

Conflict of interest

The authors declare that they have no conflict of interest.

References

1. A. Anand, M.I.U. Haq, K. Vohra, A. Raina, and M.F. Wani, Role of Green Tribology in Sustainability of Mechanical Systems: A State of the Art Survey, *Mater. Today Proc*, 2017, **4**(2), p 3659–3665
2. V.R. Rao, N. Ramanaiah, and M.M.M. Sarcar, Dry Sliding Wear Behavior of TiC-AA7075 Metal Matrix Composites, *Int. J. Appl. Sci. Eng.*, 2016, **14**(1), p 27–37
3. E. Omrani, A.D. Moghadam, P.L. Menezes, and P.K. Rohatgi, Influences of Graphite Reinforcement on the Tribological Properties of Self-Lubricating Aluminum Matrix Composites for Green Tribology, Sustainability, and Energy Efficiency — a Review, 2015
4. M. Irfan, U. Haq, and A. Anand, Dry Sliding Friction and Wear Behavior of AA7075-Si 3 N 4 Composite, Silicon, 2018 **10**(5), pp.1819–1829. https://doi.org/10.1007/s12633-017-9675-1
5. M.I. Ul Haq and A. Anand, Dry Sliding Friction and Wear Behaviour of Hybrid AA7075/Si_3 N_4/Gr Self Lubricating Composites, *Mater. Res. Express*, 2018, **5**(6), p 66544. http://doi.org/10.1088/2053-1591/aacc50
6. K.S. Vinoth, R. Subramanian, S. Dharmalingam, B. Anandavel et al., Mechanical and Tribological Characteristics of Stir-Cast Al-Si10Mg and Self-Lubricating Al-Si10Mg/MoS2 Composites, *Mater. Technol.*, 2012, **46**(5), p 497–501
7. K.P. Furlan, J.D.B. de Mello, and A.N. Klein, Self-Lubricating Composites Containing MoS2: A Review, *Tribol. Int.*, 2018, **120**, p 280–298
8. J. Lakshmipathy, S. Rajesh Kannan, K. Manisekar, and S. Vinoth Kumar, Effect of Reinforcement and Tribological Behaviour of AA 7068 Hybrid Composites Manufactured through Powder Metallurgy Techniques, *Appl. Mech. Mater.*, 2017, **867**, p 19–28
9. V. Kumar, R.K. Gautam, and R. Tyagi, Tribological Behavior of Al-Based Self-Lubricating Composites, *Compos. Interfaces, Taylor & Francis*, 2016, **23**(6), p 481–492
10. M. Vv, M.A. Joseph, and P.K. Rajendrakumar, Application of Full Factorial Design to Study the Tribological Properties of AA6061-B4C and AA6061-B4C-MoS2 Composites, *J. Tribol.*, 2018, **16**, p 71–82
11. R. Jojith and N. Radhika, Mechanical and tribological properties of LM13/TiO2/MoS2 hybrid metal matrix composite synthesized by stir casting, *Part. Sci. Technol.*, 2019, **37**(5), p 570–582
12. S.A.A. Daniel, M. Sakthivel, P.M. Gopal, and S. Sudhagar, Study on tribological behaviour of Al/SiC/MoS 2 hybrid metal matrix composites in high temperature environmental condition, *Silicon*, 2018, **10**(5), p 2129–2139
13. K. Kanthavel, K.R. Sumesh, and P. Saravanakumar, Study of Tribological Properties on Al/Al2O3/MoS2 Hybrid Composite Processed by Powder Metallurgy, *Alexandria Eng. J.*, 2016, **55**(1), p 13–17
14. P. Narayanasamy, N. Selvakumar, and P. Balasundar, Effect of Hybridizing MoS2 on the Tribological Behaviour of Mg–TiC Composites, *Trans. Indian Inst. Met.*, 2015, **68**(5), p 911–925
15. B. Rebba and N. Ramanaiah, Evaluation of Mechanical Properties of Aluminium Alloy (Al-2024) Reinforced with Molybdenum Disulphide (MOS2) Metal Matrix Composites, *Procedia Mater. Sci.*, 2014, **6**, p 1161–1169
16. M.I.U. Haq and A. Anand, Friction and wear behavior of AA 7075-Si 3 N 4 composites under dry conditions: effect of sliding speed, *Silicon*, 2019, **11**(2), p 1047–1053. https://doi.org/10.1007/s12633-018-9967-0
17. J. Hashim, L. Looney, and M.S.J. Hashmi, Metal Matrix Composites: Production by the Stir Casting Method, *J. Mater. Process. Technol.*, 1999, **92–93**, p 1–7. https://doi.org/10.1016/s0924-0136(99)00118-1

18. A. Baradeswaran and A.E. Perumal, Influence of B 4 C on the Tribological and Mechanical Properties of Al 7075–B 4 C Composites, *Compos. Part B Eng.*, 2013, **54**, p 146–152
19. A. Daoud, M.T.A. El-Khair, and A.N. Abdel-Azim, Effect of Al2O3 Particles on the Microstructure and Sliding Wear of 7075 Al Alloy Manufactured by Squeeze Casting Method, *J. Mater. Eng. Perform.*, 2004, **13**(2), p 135–143
20. S.M.J.S. Shourije and M.E. Bahrololoom, Effect of Current Density, MoS2 Content and Bath Agitation on Tribological Properties of Electrodeposited Nanostructured Ni-MoS2 Composite Coatings, *Tribol. Surfaces Interfaces*, 2019, **13**(2), p 76–87
21. K. Sekar, M. Manohar, and K. Jayakumar, Mechanical and Tribological Properties of A356/Al2O3/MoS2 Hybrid Composites Synthesized Through Combined Stir and Squeeze Casting, *Advances in Materials and Metallurgy*, Springer, 2019, p 115–125
22. M.F. Cardinal, P.A. Castro, J. Baxi, H. Liang, and F.J. Williams, Characterization and Frictional Behavior of Nanostructured Ni–W–MoS2 Composite Coatings, *Surf. Coatings Technol.*, 2009, **204**(1–2), p 85–90
23. T. Koizumi and M. Kuroda, Grain Size Effects in Aluminum Processed by Severe Plastic Deformation, *Mater. Sci. Eng., A*, 2018, **710**, p 300–308
24. J.-W. Yeh and W.-P. Liu, The Cracking Mechanism of Silicon Particles in an A357 Aluminum Alloy, *Metall. Mater. Trans. A*, 1996, **27**(11), p 3558–3568
25. H.E. Sliney, Solid Lubricant Materials for High Temperatures—a Review, *Tribol. Int.*, 1982, **15**(5), p 303–315
26. Y.-G. Cao, C.-H. Yin, Y.-L. Liang, and S.-H. Tang, Lowering the Coefficient of Martensite Steel by Forming a Self-Lubricating Layer in Dry Sliding Wear, *Mater. Res. Express*, 2019, **6**(5), p 55024
27. S.M. Sharma and A. Anand, Solid Lubrication in Iron Based Materials–A Review, *Tribol. Ind*, 2016, **38**(3), p 318–331
28. M.R. Vazirisereshk, A. Martini, D.A. Strubbe, and M.Z. Baykara, Solid Lubrication with MoS2: A Review, *Lubricants*, 2019, **7**(7), p 57
29. Z. Chen, X. He, C. Xiao, and S.H. Kim, Effect of Humidity on Friction and Wear—A Critical Review, *Lubricants*, 2018, **6**(3), p 74
30. P. Rambabu, N.E. Prasad, V. V Kutumbarao, and R.J.H. Wanhill, Aluminium Alloys for Aerospace Applications, *Aerospace materials and material technologies*, Springer, 2017, p 29–52
31. N.N. Gosvami, J.A. Bares, F. Mangolini, A.R. Konicek, D.G. Yablon, and R.W. Carpick, Mechanisms of Antiwear Tribofilm Growth Revealed in Situ by Single-Asperity Sliding Contacts, *Science*, 2015, **348**(6230), p 102–106
32. B. Chen, J. Zhang, J. Jia, W. Hu, and C. Gong, Tribological Properties of Solid Lubricants (Graphite, MoS2) for Ni Based Materials, *IOP Conf. Ser. Earth Environ. Sci.*, 2018, **186**, p 12030
33. H. Singh, M.I.U. Haq, and A. Raina, Dry Sliding Friction and Wear Behaviour of AA6082-TiB_2 in Situ Composites, *Silicon*, 2019, **12**, p 1469–1479. https://doi.org/10.1007/s12633-019-00237-y
34. M.V. Hosur, M. Adbullah, and S. Jeelani, Studies on the Low-Velocity Impact Response of Woven Hybrid Composites, *Compos. Struct.*, 2005, **67**(3), p 253–262
35. C.S. Ramesh and M. Safiulla, Wear Behavior of Hot Extruded Al6061 Based Composites, *Wear*, 2007, **263**(1–6), p 629–635
36. A.R. Riahi and A.T. Alpas, The Role of Tribo-Layers on the Sliding Wear Behavior of Graphitic Aluminum Matrix Composites, *Wear*, 2001, **251**(1–12), p 1396–1407
37. B. Venkataraman and G. Sundararajan, Correlation between the Characteristics of the Mechanically Mixed Layer and Wear Behaviour of Aluminium, Al-7075 Alloy and Al-MMCs, *Wear*, 2000, **245**(1–2), p 22–38